The growth and superconducting properties of RE–Ba–Cu–O single grains with combined RE elements (RE = Gd and Y)

Yunhua Shi [ORCID], Giovanni Bergamo-Andreis, Anthony R Dennis, John H Durrell [ORCID] and David A Cardwell

Engineering Department, University of Cambridge, Trumpington Street, Cambridge, CB2 1PZ, United Kingdom

E-mail: ys206@cam.ac.uk

CrossMark

Abstract

The superconducting properties, melting temperatures and crystal growth rates of single grain, RE–Ba–Cu–O [(RE)BCO] bulk superconductors (where RE = a rare earth element or yttrium) decrease with the RE-element sequence of Nd, Sm, Eu, Gd, Dy and Y. The mechanical properties of these technologically important materials, on the other hand, however, improve in the same sequence. Consequently, one promising approach for optimising the balance between mechanical and superconducting properties of bulk (RE)BCO superconductors, or for adjusting growth rate, is the use of combinations of different rare earth elements. In this study, we explore combinations of Gd and Y in the formation of (Gd–Y)–Ba–Cu–O single grains. We describe the optimisation of the growth process for this multi-RE element system and use optical and scanning electron microscopy to study the microstructure of both non-superconducting $(Gd–Y)_2BaCuO_5$ [(Y–Gd)-211] phase inclusions and the $(Y–Gd)Ba_2Cu_3O_{7-\delta}$ [(Y–Gd)-123] phase matrix itself. We demonstrate that (Gd–Y)–Ba–Cu–O single grains can be fabricated reliably and that they exhibit reasonably good superconducting properties. We observe that there is an increase in RE-211 particle size in this mixed rare earth system, which, ultimately, limits sample performance, and conclude that this may be a general disadvantage of this approach to the synthesis of single grains for high field engineering applications.

(Some figures may appear in colour only in the online journal)

Introduction

Bulk (RE)–Ba–Cu–O [(RE)BCO] superconductors, consisting of a $REBa_2Cu_3O_{7-\delta}$ (RE-123) phase matrix containing RE_2BaCuO_5 (RE-211) inclusions (where RE is a rare earth element such as Nd, Sm, Eu, Gd, Y, Yb) can generate trapped magnetic fields that are up to ten times higher than the maximum fields obtainable in conventional, Fe-based permanent magnets [1–3]. Unfortunately, the presence of grain boundaries in (RE)BCO bulk superconductors results in an exponentially decreasing critical current density (J_c) [4,5] as the grain boundary misorientation angle is increased. Consequently, bulk RE–Ba–Cu–O containing grain-boundaries exhibit significantly reduced J_c [6,7]. As a result, in order to achieve good superconducting properties, it is necessary to fabricate (RE)BCO bulk superconductors in the form of a large, single grain (i.e. a quasi-single crystal).

The process of fabricating single grain, (RE)BCO bulk samples is relatively complex [8], and is based usually on the

1

so-called top-seeded-melt-growth (TSMG) [9] technique. TSMG involves heating a precursor pellet consisting of a mixture of RE-123 and RE-211 powders to a temperature above the peritectic temperature of the (RE)BCO system to fully decompose the RE-123 phase into RE-211 and a liquid phase ($Ba_3Cu_3O_8$). Subsequent nucleation of a single grain is achieved by placing a seed at centre of the top surface of the pellet and slow-cooling the seed/pellet arrangement back through the peritectic temperature. The peritectic reaction then reverses under these conditions ($RE_2BaCuO_5 + Ba_3Cu_5O_8$ (liquid)$\rightarrow$$REBa_2Cu_3O_{6.5}$) and a single grain forms that consists of a continuous RE-123 phase matrix containing embedded RE-211 precipitates due to the combined effects of an excess of RE-211 phase introduced originally to the precursor powder and to an incomplete peritectic reaction. The signatures of the successful growth of a single grain are (i) the presence of four-fold crystallographic facet lines on the upper surface and sides of the as-grown sample without the presence of visible sub-grains and (ii) a single peak in the measured trapped field distribution of a fully magnetised sample.

It is possible to fabricate (RE)BCO from a mixture of rare earth elements. ($Nd_{0.33}Eu_{0.33}Gd_{0.33}$)$Ba_2Cu_3O_y$ [(NEG)-BCO] samples melt-processed in reduced O_2 in Ar were first reported in 1999 with very high critical current densities, J_c's, of 7.5 A m^{-2} at 77 K in zero magnetic field and J_c 6.8 A m^{-2} [10] in a magnetic field of 2.5 T. These values were approximately double those reported elsewhere at that time [2]. The trapped field of a NEG-BCO sample of diameter 38 mm was reported subsequently to have reached 1.38 T at 77 K in 2003 [11]. Mixed rare earth systems of Sm combined with either Eu [12] or Nd [13], or Nd combined with Eu [14] have also been grown successfully in the form of single grains. YBCO systems doped with a small amount of Y and Dy or Gd or Sm [15] exhibit improved J_c [16,17] compared to the corresponding single-element (RE)BCO system. Large, single-grain (Gd,Y)BaCuO superconductors fabricated by the RE compositional gradient technique [18] suggest that the mechanical properties of GdBCO, YBCO and (Gd–Y)BCO are similar. (Gd–Y)BCO thin films and tapes [19,20] have also exhibited improved J_c compared to pure, single element (RE)BCO compositions, as have other tapes composed of mixed RE elements [21]. It should be noted, however, that the flux pinning mechanism in tapes and thin films almost certainly differs significantly from that in bulk, single grain materials, which is determined primarily by the size and distribution of RE-211 inclusions embedded within the bulk microstructure (which, in general, are not present in tapes and thin films).

Although the work conducted on mixed rare earth systems described above indicate that these systems can exhibit better J_c's than single-element rare earth samples, more recently the development of RE bulk superconductors incorporating only Y or Gd rare earth elements has achieved $J_c(0)$ values in excess of 10 kA m^{-2} [22–24] at 77 K with corresponding increases in record levels of trapped magnetic field [25,26], exceeding the reported historical performance of mixed rare earth samples.

The superconducting properties at 77 K, growth rates and melting temperatures of RE–Ba–Cu–O single rare earth element bulk superconductors decrease as the RE is changed in the sequence Nd, Sm, Eu, Gd, Dy and Y [16,21]. Significantly, however, the mechanical properties of the single grain samples improve in the same sequence. We postulate, therefore, that employing a mixture of rare earth elements could improve the mechanical performance of these technologically important materials, even if their superconducting performance is not enhanced significantly.

The substitution of light rare earth element (LRE) onto the Ba site in mixed LRE bulk superconductors can lead to a significant deterioration in T_c and J_c [27]. However, $YBa_2Cu_3O_{7-\delta}$ (Y-123) is a stoichiometric compound and, whilst there a small amount of Gd/Ba substitution in $GdBa_2Cu_3O_{7-\delta}$ (Gd-123) during processing, it is not severe. Consequently, the (Gd–Y)BCO system is selected here to allow a study of the effect of using mixtures of rare earth elements where the interpretation is not complicated by the effects of substitution. Moreover, melt-processing of the (Gd–Y)BCO system has not been studied previously and extensively over a full chemical range and under an air processing atmosphere.

The main conclusion from previous studies is that superconducting systems containing mixed RE elements have better superconducting properties, although predominantly in the values of local J_c measured by magnetic techniques. Improved trapped field, however, which is a more practical property for realising applications of single grain, bulk (RE) BCO superconductors, have not been reported generally in these materials. J_c actually fluctuates significantly from sample to sample and varies considerably with position even within one single grain [28,29], and is, therefore, not an accurate and definitive measure of the superconducting quality of a single grain. As a result, we have measured both local T_c and J_c at 4 positions in each sample and the trapped fields of 26 samples fabricated in this study.

In this paper, we address the challenges to achieve single grain growth for the (Gd–Y)BCO system by considering the growth process parameters, including optimisation of the heating profile through differential thermal analysis (DTA). The superconducting properties, T_c, J_c and trapped field of five different relative proportions of Y and Gd are measured and we report optical and scanning electron microscope analysis of both the single grain matrix and embedded precipitates. Finally, we comment on the prospects for improving the overall performance of bulk superconductors fabricated from mixed rare earth elements.

Experimental

Raw powders of Gd-123, Y-123, Gd-211 and Y-211 were sourced from Toshima. The powders were of 99.9% purity and with the following grain sizes: Gd-123 and Y-123, 2–3 μm; Gd-211 and Y-211, 1–2 μm. The two base standard powders used were GdBCO or YBCO powders in
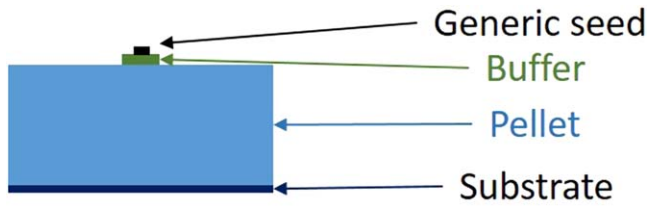
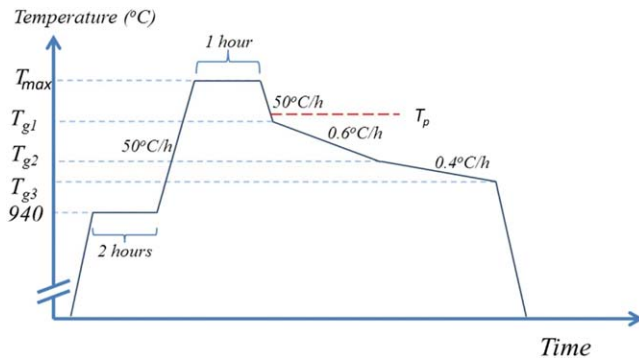**Figure 1.** Schematic illustration of the arrangement of the superconducting pre-forms used for melt processing.

Figure 2. Representative heating profile used to melt-process the single grains in this study.

compositions 75 wt% $GdBa_2Cu_3O_{7-\delta}$ (Gd-123) (or Y) + 25 wt% Gd_2BaCuO_5 (Gd-211)(or Y) + 0.5 wt%CeO_2.

Powders with a variable Y:Gd element weight ratio were also prepared from the two base standard powders as follows; 100:0, 75:25, 50:50, 25:75 and 0:100. These systems are labelled in this paper as YBCO, Y75Gd25BCO, Y50Gd50BCO, Y25Gd75BCO and GdBCO, respectively. Five compositions of four bulk superconducting pellets, each of mass 10 g, were prepared in the arrangement illustrated schematically in figure 1. A generic seed [30] was placed at the centre on the top of a buffer pellet, which, in turn, was placed on the top surface of each green, uniaxially pressed sample [31,32]. A substrate consisting of a liquid-rich phase [33,34] was used to prevent the nucleation and growth of sub-grains at the bottom of the samples and to supply some liquid $Ba_3Cu_5O_8$ back to the growing pellet.

Four samples, each of the same composition, were heated in air in a furnace with a temperature profile shown in figure 2. A number of key temperatures, such as a two-hour holding period at 940 °C to promote consolidation, were maintained constant for all samples. Others, including the melting temperature, T_m, the initial growth temperature, T_{g1}, T_{g2} and final growth temperatures T_{g3}. were adjusted for each composition based on the results of DTA of the individual precursor powders. The DTA analysis of a powder mixture of mass approximately 100 mg was performed using a LABSYS Evo device manufactured by Setaram.

Two sets of samples were produced as part of this study. In the first set, samples containing a single rare earth element, YBCO and GdBCO, were fabricated using existing optimised heating profiles; the other three mixed rare earth systems were fabricated using a slower heating profile to avoid the formation of sub-grains.
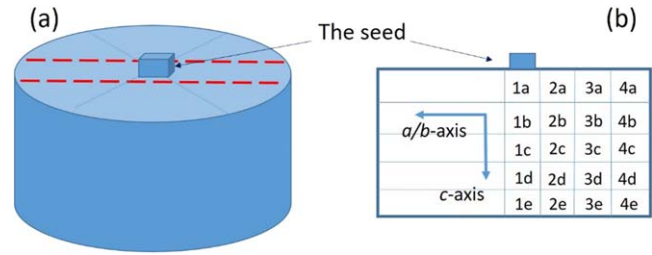

Figure 3. (a) Schematic illustration of a single grain and (b) the notation used to define the positions of the sub-specimens in the parent single grain used to measure T_c and J_c.

The second set of samples of composition Y75Gd25BCO, Y50Gd50BCO and Y25Gd75BCO were fabricated using faster heating profiles with the aim of reducing the RE-211 particle size and minimising liquid phase loss during the melt process.

The as-grown single grains were annealed in a tube furnace in an oxygen atmosphere at 450 °C–400 °C for 7 days to allow oxygen to diffuse into the single grains and convert their lattice structure from tetragonal to orthorhombic, which is the superconducting phase [35].

The trapped field of each single grain was measured by cooling the sample to 77 K in a field of 1.4 T, and then removing the field over a linear, 100 s ramp. A hand-held Hall probe was placed 0.5 mm above the top surface of each sample in order to locate the position of the maximum trapped magnetic field. The complete trapped field profile was measured using a rotating array of eighteen probes placed 1.5 mm above the sample surface.

A thin slab was cut from the centre of the sample with the largest trapped field of each composition, as shown schematically in figure 3(a), which was then cut further into sub-specimens of approximate dimensions 3 mm, 2 mm and 1 mm in the *a*, *b* and *c* lattice directions, respectively. Sub-specimens at positions 1a, 3a, 1d and 3d, also shown schematically in figure 3(b), were analysed using a superconducting quantum interference device magnetometer (SQUID: Quantum Design MPMS-XL) to determine the magnetic moment and the magnetic hysteresis loop as a function of temperature for each specimen. Critical current density was calculated from the magnetisation loops using the extended Bean model [36]. The sample microstructure was examined using an optical microscope (Nikon Eclipse ME 600 with an attached Moticam camera at magnifications 50× and 1000×) and a scanning electron microscope (using Carl Zeiss EVO LS-15) at 1 mm intervals along the axis of rotational symmetry, which included a facility for energy dispersive x-ray spectroscopy (Phillips XL-30).

Results and discussion

Peritectic temperatures and the heating profiles for the first set of samples

It is possible to grow (RE)BCO bulk samples by heating a polycrystalline bulk precursor above its peritectic
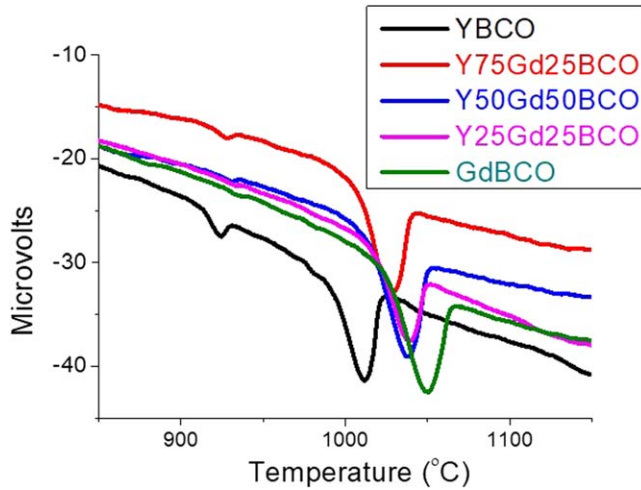
Figure 4. Differential Thermal Analysis of the 5 different precursor powder compositions under investigation.
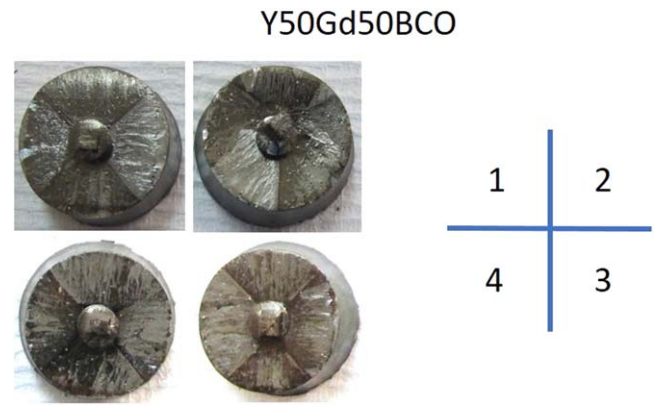

Figure 5. Single grains (16 mm in diameter) fabricated with a Y:Gd ratio of 50:50 in the first sample set.

Table 1. Temperature parameters selected for samples of different compositions.

Y_{123}: Gd_{123}	Set	T_{max} (°C)	T_{g1} (°C)	T_{g2} (°C)	T_{g3} (°C)
100:0	I	1057	1012	997	977
75:25	I	1065	1030	1010	985
50:50	I	1070	1035	1015	990
25:75	I	1080	1040	1020	995
0:100	I	1080	1040	1030	1005
75:25	II	1067	1022	1014	987
50:50	II	1072	1032	1020	995
25:75	II	1080	1042	1030	1005

decomposition temperature. The sample is then allowed to cool from a temperature that is sufficiently high, with spontaneous nucleation and subsequent single grain growth being initiated from a seed crystal with a higher melting temperature than the system being fabricated. For the YBCO system, the peritectic reaction during the crystal growth is: $Y_2BaCuO_5 + Ba_3Cu_5O_8 + \delta O_2 \rightarrow 2YBa_2Cu_3O_{6.5+\delta 1}$ ($0 < \delta < 0.5$), which takes place at about 1010 °C. The peritectic reaction during the crystal growth process for the GdBCO system is: $Gd_2B_1Cu_1O_5 + Ba_3Cu_5O_8 + \delta O_2 \rightarrow 2Gd_1Ba_2Cu_3O_{6.5+\delta}$ ($0 < \delta < 0.5$), which occurs at about 1050 °C.

It is necessary to determine the peritectic reaction temperature of the combined Y–Gd rare-earth systems in order to achieve successful single grain growth, and this can be achieved conveniently and routinely using DTA. Figure 4 shows the DTA analysis of the peritectic reactions of the five different compositions under investigation. The results show that the combined Y:Gd precursor powders each exhibit a single peritectic transition temperature, which increases with increasing Gd content. The single peak indicates that the composition behaves as a single phase, rather than as a simple mixture of YBCO and GdBCO, which is positive from a processing perspective.

The heating profiles used for the growth of single grains were adjusted based on the change in peritectic temperature observed in the DTA analysis, with the systemic changes in temperature for each composition shown in table 1. The maximum temperature T_{max} in the heating profile was selected to be 40 °C above the peritectic temperature, determined by DTA, in order to ensure that the RE-123 fully decomposed to RE-211 and $Ba_3Cu_5O_8$. The samples were heated at 100 °Ch^{-1} to 940 °C, and stabilised at this temperature before being heated at 50 °Ch^{-1} to the T_{max}. This temperature was maintained for an hour and then decreased to T_{g1}. The sample cooling rate was then reduced to 0.6 °Ch^{-1} until temperature T_{g2} was reached, and then to 0.4 °Ch^{-1} until T_{g3}, before being cooled rapidly at 100 °Ch^{-1} to room temperature.

20 single grains were grown as part of set I for the two sets of samples. A further 6 samples were grown subsequently in the second set using different heating profiles.

Growth of single grains

Figure 5 shows the typical appearances of the samples fabricated in this study (the 4 samples were placed in the furnace in positions 1 to 4, as shown). Y50Gd50BCO samples at positions 1, 3 and 4 grew successfully into single grains, although the sample at position 2 failed as a result of the seeding process. The four-fold facet lines, which are indicators of successful grain growth, could be seen clearly in most of the samples. The failure rate of these samples was no different from that experienced typically for single RE element bulk superconductors (i.e. corresponding to a yield of 85% in the first sample set).

The distribution of the magnitude of trapped field in the *z* direction measured along the *x* and *y*-axes of a single grain should be conical, given that the slope of the flux profile is defined by $dB/dx = \mu_o J_c$. This is reflected typically in the trapped field profile if the sample growth has resulted in the formation of multiple grains, in which case the distribution of trapped field exhibits multiple peaks. Figure 6(a) shows an example of the trapped field distribution in the *z* direction using the 4th sample, with composition of Y50Gd50BCO.
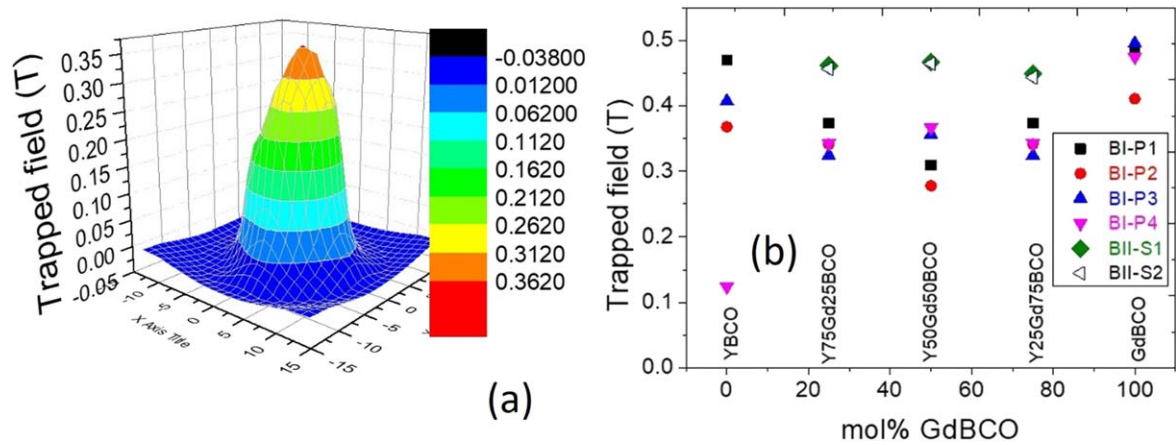
Figure 6. Trapped fields of the samples containing Y and Gd (a) A typical trapped field profile (in this case for the 4th sample with the composition of Y50Gd50BCO) (b) Maximum trapped field of each bulk sample fabricated in Sets I and II as a function of molar content of GdBCO.
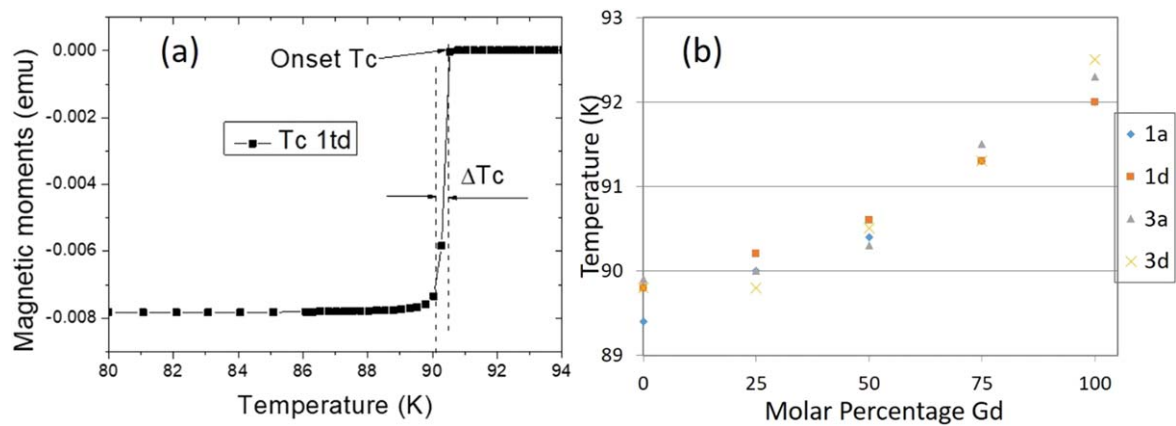

Figure 7. (a) A typical M(T) data set measured by SQUID magnetometry showing the onset, offset and width definitions of the transition to the superconducting state. (b) Onset T_c of specimens at different positions of the single grain with different concentrations of Gd and Y.

Refinement of set production after review of the superconducting properties.

The maximum value of the trapped field indicates the quality of the single grain since it is proportional to average critical current density (J_c) within the bulk of the sample. Figure 6(b) shows the maximum trapped field value of each composition of 4 samples at positions of 1 to 4 (BI-P1 to BI-P4) fabricated in the first set. It can be seen that the maximum trapped field of the combined element rare earth samples is, on average, lower than that of the pure samples, YBCO and GdBCO when the properties of the samples fabricated at positions 1 to 4 in the first set are compared directly. The trapped fields measured in samples of a given composition are relatively consistent. The outliers (sample 2 of 100% Gd and sample 4 of 0% GdBCO) exhibit trapped fields that are significantly inferior to the other samples, which is due to the seeding issues discussed earlier.

Figure 7 shows the critical superconducting transition temperature (T_c) of the samples exhibiting the highest trapped fields for each initial powder composition, as measured by SQUID magnetometery. The measurement of critical temperature, T_c, was achieved by the measurement of magnetic

moment as a function of temperature, as shown in figure 7(a), in a small applied field of 0.002 T. The onset T_c is the temperature at which the sample loses its magnetic moment, whilst the offset T_c is the temperature at which the magnetic moment starts to decrease. ΔT_c is defined as the temperature difference corresponding to that between the onset T_c and 90% of the offset T_c, as shown in figure 7(a). The T_c and ΔT_c of the standard YBCO and GdBCO samples are similar to those reported previously [37,38]. T_c of the samples with combined Y and Gd elements all exhibit a single transition in their T_c-temperature curves, which indicates the presence of a single superconducting phases in these samples [(Y–Gd)-123]. T_c appears to increase monotonically as the proportion of Gd is increased, as shown in figure 7(b). The ΔT_c, of all specimens of all compositions in the study is less than 1 K, which indicates that the systems with combined Gd and Y do not suffer significantly from the effects of Gd/Ba substitution in the RE-123 phase matrix.

The magnetic moments of specimens at positions 1a, 3a, 1d and 3d in the first set samples with the highest trapped fields were analysed using SQUID magnetometry and J_c was calculated using the extended Bean model using the data from the magnetic hysteresis loops for each sub-specimen. J_c was
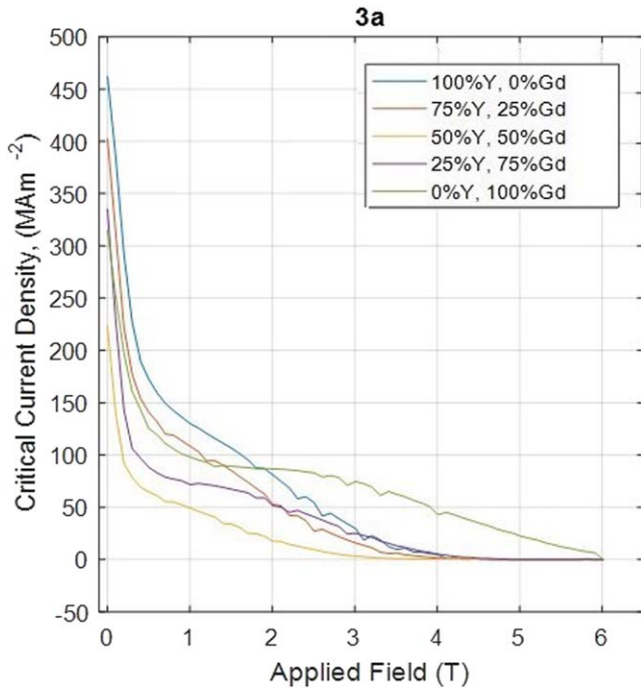
Figure 8. J_c–B curves of the sub-specimens at positions 3a for 5 different compositions.

Figure 9. Second set of samples, 16 mm in diameter, fabricated using faster heating profiles.

Figure 10. Heating profiles of two sets of the samples produced in this study.

observed to fluctuate from position to position within one single grain and J_c did not increase with the addition of YBCO to GdBCO or with the addition of GdBCO to YBCO, as can be seen from the J_c–B curves measured at sub-specimen positions 3a in figure 8. It is clear, however, that the J_c values of the sub-specimens with combined Gd and Y elements are smaller than those of either pure YBCO or GdBCO and there is no pronounced 'peak' effect in all these samples. This suggests that a combination of rare earth elements does not improve either J_c or trapped field.

Figure 6(b) shows that (RE)BCO systems from the first set of combined Gd and Y exhibit lower trapped fields than either single-rare element composition. It is clear that the values of the average J_c of the first set of samples with combined Gd and Y are relatively low. We can conclude, therefore, that the combined element systems do not suffer significantly from the effects of Gd/Ba substitution because all values of ΔT_c lie within 1 K. This suggests that one of the factors that limit J_c is the size, number and distribution of flux pinning centres in this study, but not the T_c and ΔT_c of the samples. Pinning centres are microstructure-related parameters, which, in turn, can be controlled by adjusting the material processing parameters, such as heating profile. The addition of Gd-123 and Sm-123 powders to YBCO to grow single grains requires a refinement of the TSMG heating profile, which is consistent with the report of Volochová *et al* [15]. For this reason, a second set of combined (Gd–Y)BCO single grain samples were produced in order to compare the properties of the further refined samples to those of pure YBCO and GdBCO. The second set of single grain samples, 16 mm in diameter, for compositions containing a
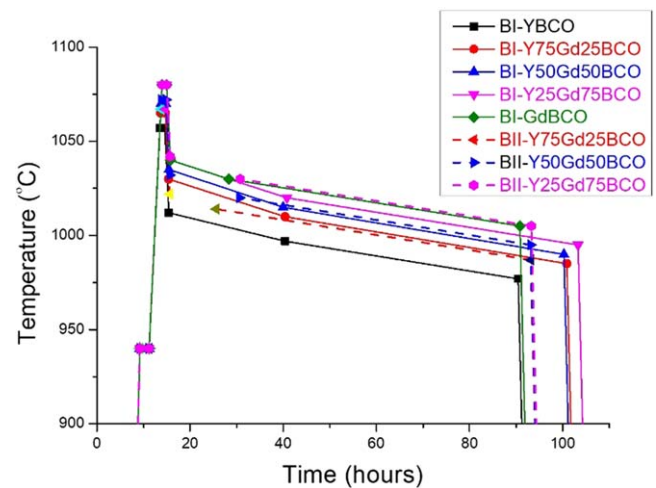
combination of Y and Gd elements were fabricated, therefore, using a more rapid heating profile.

Figure 9 shows two samples of each composition fabricated in the second set, 16 mm in diameter. The maximum trapped field is indicated at the top of each photograph. Figure 10 shows the heating profiles of all the samples in the two sets. The newly adjusted values of T_{g1}, T_{g2} and T_{g3} for samples BII-S1 and BII-S2, processed with combined Y and Gd are also shown in table 1. It can be seen that the new heating profiles for the samples with compositions Y75Gd25BCO, 50Y50GdBCO and Y2575GdBCO are shorter than that used for the first set for the equivalent samples. An attempt to fabricate more samples was made in the second set than is represented in figure 9, although the failure rate was higher due to the much faster heating profiles, which resulted in the more frequent formation of sub-grains. Although the use of a slower cooling rate leads generally to more steady single grain growth [39], as evidenced by the initial attempt to grow a large number of (RE)BCO single grains with combined Gd and Y elements in different proportions, this may lead to increased liquid loss [40] and to an
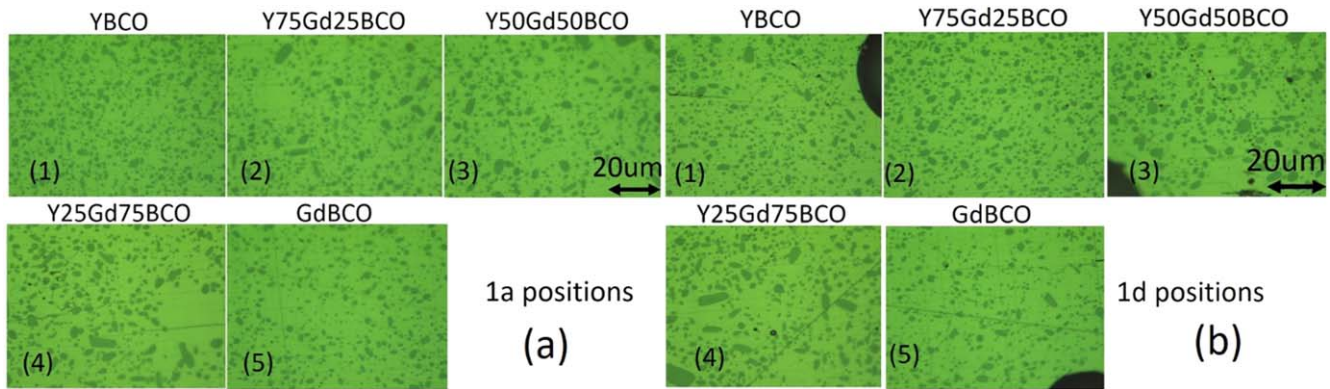
Figure 11. (a) Photographs of the microstructure of the samples with the compositions indicated at positions 1a and (b) photographs of the microstructures of the samples with the composition at positions 1d, with distance through the thickness of the sample.
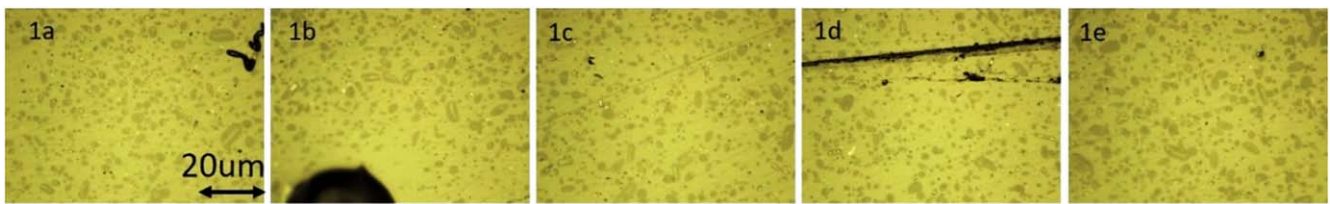

Figure 12. Photographs of the microstructures of sample Y50Gd50BCO at positions 1a to 1e.

increase in the size of RE-211 inclusions in the microstructure. The combined effects of these processes lead directly to lower values of J_c and to a reduction in the maximum value of trapped field.

The maximum trapped fields of the second set of samples (BII-S1 and BII-S2) in figure 9 are indicated in figure 6(b) by green diamonds and navy triangles, within the blue dashed line. It can be seen that the trapped fields of samples 1 and 2 in the second set, BII-S1 and BII-S2, are higher compared to samples in the first set, BI-P1 to BI-P4, of the same composition, suggesting that adjusting the heating profiles improves the trapped field of these samples. As a result, all samples at this stage exhibited a similar trapped field following refinement of the heating profile of the samples with combined Y and Gd elements, with additional improvements anticipated with further optimisation.

Microstructural analysis

It was reported that J_c in (RE)BCO bulk superconductors varies in proportion to volume fraction of RE-211 [24], although the particle size of RE-211 might be too large to work effectively as pinning centres in some RE compositions. Therefore, the microstructures related to RE-211 were examined in detail using an optical microscope and SEM.

Figure 11 shows the microstructures of the samples of different compositions at a magnification of ×1000. Figures 11(a) and (b) show photographs of sub-specimens at positions 1a and 1c or 1d, respectively. The photographs of the YBCO (figure 11(a(1))) and GdBCO (figure 11 (a(5))) samples at positions 1a and 1c (figures 11(b(1)) and 10(b(5)), respectively) demonstrate clearly that the matrix is either Y-123 or Gd-123 and that the inclusions are Y-211 and

Gd-211. The size and distribution of the Y-211 or Gd-211 particle inclusions is typical for these singe element, single grain compositions. Usually the distribution of RE-211 follows a trend described by particle pushing/trapping theory [41], which predicts very few RE-211 particles in the vicinity of the seed, but with an increasing concentration and particle size of RE-211 inclusions as the distance from the seed increases. The reasonably large quantity of Y-211 or Gd-211 at the positions immediately beneath the seed (position 1a figure 11(a)) is expected due to the use of a buffer pellet [8,31]. In this case, the effective area beneath the seed extends into the buffer, and the differences in RE-211 particle inclusions features between photographs taken at positions 1a and at 1tc (or 1d) are, therefore, smaller.

However, it is interesting to see in the photographs of the samples containing a combination of Y and Gd (figures 11(a (2))–(a(4)), (b(2))–(b(4))) the presence of large, circular inclusions, which become larger when the composition of Gd is increased. Overall, the number of inclusions in these images is smaller than in those of either YBCO or GdBCO. A possible explanation for this is that the RE-211 particles are larger when slower heating profiles are employed due to Ostwald ripening in the Ba–Cu–O liquid [42] that occurs at elevated temperature. Therefore, the microstructures of the single grains fabricated in the second set of samples were also examined. Figure 12 shows the microstructures at a magnification of ×1000 of the sample with composition Y50Gd50BCO melt-processed in the second set at different positions along the *c*-direction from positions 1a to 1e. Comparing with the sample fabricated in the first set at positions 1a (figure 11(a(3))) and 1d (figure 11(b(3))), it can be seen that the large inclusions still exist but are fewer in number. In addition, the shapes of these large inclusions are
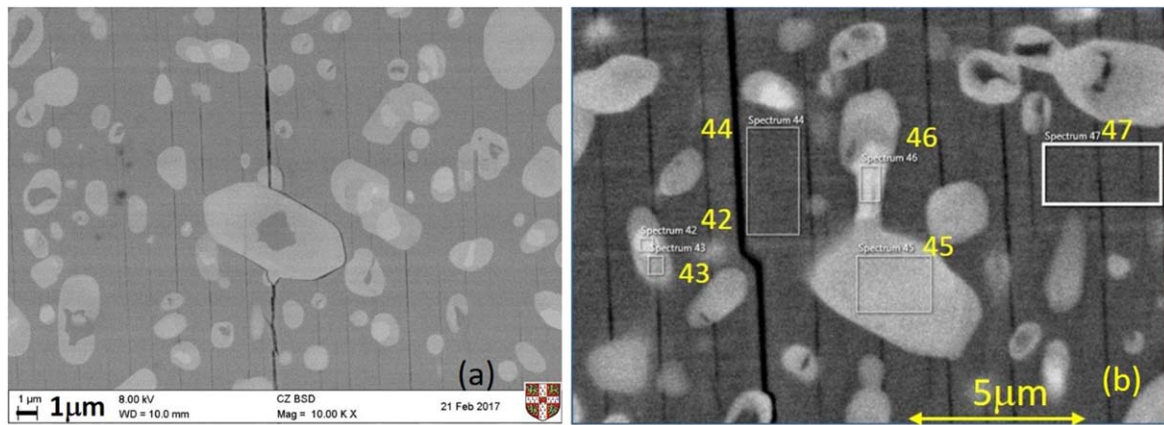
Figure 13. (a) Back-scattered diffraction image of the microstructure of sample Y25Gd75BCO and (b) The same sample under higher magnification.

Table 2. EDX spectra of the sample 25Y75GdBCO in figure 13(b).

Areas	Description	O (at%)	Cu (at%)	Y (at%)	Ba (at%)	Ce (at%)	Gd (at%)	Gd+Y (at%)	Total (at%)
42	Bright area inclusion	55.25	13.59	3.26	12.74	0.12	15.04	18.3	100
43	Grey Inclusion	55.59	12.91	5.63	12.69	0.08	13.11	18.74	100.01
44	Dark Area/Matrix	52.52	21.95	3.05	16.34	0	6.15	9.2	100.01
45	Grey inclusion	55.54	11.22	6.78	11.89	0.24	14.33	21.11	100
46	Bright area bridging two greys	55.14	13.13	3.65	12.88	0.05	15.2	18.85	100.05
47	Dark Area/Matrix	52.37	21.53	3.37	16.06	0.16	6.5	9.87	99.99

more irregular and are not very circular, and a greater number of smaller particles are present. J_c is highly dependent on the single grain microstructure and is proportional, in general, to the volume fraction of the RE-211 particle present (at least for relatively low RE-211 concentrations). The composition of RE-211 is fixed in the precursor, and J_c increases, in general, both with increasing RE-211 density and decreasing RE-211 particle size [22,24,43]. The time used to grow the second set of samples was reduced roughly by 10 h, which can be seen in figure 10, and this leads to a reduced average size of RE-211 inclusions and therefore to an improved average J_c and, in turn, to improved trapped fields.

Chemical compositions of the matrix and the inclusions of the single grains containing combined Y and Gd

The microstructure and composition of the sample with combined Y and Gd was analysed using an SEM with a back-scatter detector and Energy-dispersive x-ray spectrometer (EDX). Figure 13(a) shows the general features of these samples with combined RE elements. It can be seen from the contrast of the images that the inclusions do not have a uniform chemical composition. Some particles have a single colour (which suggests a single composition), whereas others have either a lighter or darker core within their interior. EDX was used to determine the relative concentration of chemical elements present in each sample in an attempt to understand the approximate chemical composition of the selected areas, as shown in figure 13(b).

The results of EDX on all 3 samples fabricated with combined Y and Gd indicate that the matrix contains both Y and Gd elements when the precursor contains both Y and Gd. Table 2 shows an example of the results obtained for sample 25Y75GdBCO. This suggests that the matrix of the sample contains both Y and Gd elements (spectra 44 and 47) and that the chemical formula approximately to RE(Y–Gd)-123. The matrix has been established to be superconducting from the supporting T_c and J_c measurements, suggesting it to be the superconducting, orthorhombic RE-123 phase. The single T_c transition and single peak in present in the DTA curve suggests further that (Y–Gd)-123 is, indeed, a single phase. The composition of (Y–Gd)-123 is relatively uniform according to these results (spectra 44 and 47). However, the Gd element is the more dominant composition (roughly Gd:Y = 2:1 in atomic ratio) in the matrix, which is lower than the overall composition of Gd in the sample in figure 13(b) Y25Gd75BCO.

The results of EDX also suggest that the inclusions are not simple RE-211 particles. The light region in the inclusions are rich in Gd (spectra 42 and 46) and the dark regions are rich in Y (not shown in this figure). Therefore, the inclusions in the samples with combined Y and Gd could be either Y-211, or Gd-211 or (Y–Gd)-211 with a Gd-211 or Y-211 core. Every particle could be of a different composition with a general formula of (Y–Gd)-211, which is consistent with spectra 42, 43, 45 and 46. The Gd element is a more dominant composition due to the overall composition of Gd in the sample in figure 13(b) Y25Gd75GdBCO, although the atomic

proportion between Gd and Y changes from Gd: Y $\cong$ 5: 1 [spectra 42 (15.04 : 3.26) and 46 (15.2 : 3.65)] to 2: 1 [spectra 43 (13.11 : 5.63) and 45 (14.33 : 5.63)].

The presence of a combination of Gd and Y in discrete phases, and regions that are Gd-rich or Y-rich within the RE-211 particles is similar to that found in the other two systems (Y75Gd25BCO and Y50Gd50BCO). The same phenomenon has also been reported in combined-element (Dy, Y)BCO bulk superconductors [16]. The divergence of the composition of the (Y–Gd)-211 inclusions and the precursor powder 25YGd75BCO may be because the growth of a single grain with a combination of rare earth elements is not exactly the same as the growth of a system only containing one rare earth element, such as Y or Gd.

Both Y-123 and Gd-123 phases decompose to Y-211 + $Ba_3Cu_5O_8$ and Gd-211 + $Ba_3Cu_5O_8$ when the pellets are heated up to T_m. The DTA results show that there is only one peak associated with these systems, suggesting that the chemical reaction at the equilibrium state should be (Y + Gd)-123 (i.e. one single phase), which is the same as that observed by mixing Nd, Eu with Gd [27,44] and by mixing Nd with Eu over the full compositional range [14]. (Y + Gd)-123 then decomposes peritectically to form (Y–Gd)-211 + $Ba_3Cu_5O_8$, with the proportion of the Y + Gd being the same as that within the precursor powder. A longer holding time at T_m helps the system to reach the equilibrium state. However, it is not possible to maintain the decomposed sample at T_m for an extended period due to the loss of liquid during the single grain fabrication process. The phases present at T_m are (Y + Gd)-211, $Ba_3Cu_5O_8$ and Y-211 and Gd-211 given that extra Y-211 and Gd-211 was added to the precursor powder, with the particle size of the added, single-element RE-211 compositions influencing significantly that in the sample microstructure. The (Y + Gd)-211 present at T_m, however, arises from the decomposition of the (Y + Gd)-123 phase, which might originate from either Y-123 + Gd-123 or $Ba_3Cu_5O_8$ + (Y-211 + Gd-211) in the raw materials. The existence of three distinct types of RE-211 phase in the system with combined rare earth elements is the main difference compared to single-element RE systems.

Reversal of the peritectic reaction initiates single grain growth on cooling;

$$(Y - Gd) - 211 + Ba_3Cu_5O_8 \rightarrow (Y + Gd) - 123$$
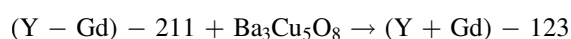
with the remaining (Y + Gd)-211, Y-211 and Gd-211 coalescing to form either single phase Y-211 or Gd-211, or a cored structure. As a result, the probability of growth into a larger RE-211 particle is greater than in a (RE)BCO system containing a single RE element. These inclusions are ultimately trapped within the solid RE-123 phase matrix. We can also see that the pushing/trapping effect is not apparent in figure 12 given that the RE-211 particle sizes and distributions look very similar across positions 1a to 1e. This is confirmed by the J_c–B curves, which also fail to exhibit a significant trend, as described earlier. The reason might be that the RE-211 particles, which cannot be treated effectively as inert particles in a multi RE element composition, are no longer being pushed/trapped, but instead grow onto each other.

It was also observed that the number of (Y–Gd)-211 inclusions in figures 12 and 13 are lower than is observed typically for Y-211 or Gd-211 in standard, single-RE element YBCO or GdBCO. This is because the nucleation sites for the RE-211 particles, which form from the decomposition of the RE-123 phase at a pro-peritectic (melting) stage, are fewer. The number of nucleating sites is determined mainly by the concentration of the RE-211 phase in the precursor powder [10]. The $Ba_3Cu_5O_8$ flux (i.e. the liquid phase that dissolves Y or Gd) formed at T_m is essentially the same for all compositions investigated, given that the ratio of the molar percentage of the RE-123 and RE-211 phases is the same in each case. This yields a reduced number of nucleating sites and, therefore, makes the growth of RE-211 particles easier, compared to pure YBCO or GdBCO.

In summary, the compositional analysis of the RE-123 phase matrix and inclusions within samples containing both Y and Gd suggests that these elements can co-exist either in the matrix and within RE-211 inclusions. However, the RE-211 inclusions in single grains containing both Y and Gd are fewer and larger compared to pure YBCO or GdBCO, which explains potentially why the multi-RE element single grains exhibit lower trapped fields. (Note that flux pinning in tapes and thin films is likely to differ significantly from that in bulk materials given the general absence of RE-211 inclusions in the former.)

Conclusions

Mixed rare earth single grain superconductors containing Y and Gd have been grown successfully with a range of compositions. This was achieved by via DTA analysis to optimise the heating profile used during the top seeded melt growth process.

Significantly, the presence of a single DTA peak in the peritectic decomposition of every ratio of (Y + Gd)BCO studied in this investigation suggests that Gd and Y act consistently as a single phase in the (RE)BCO composition. As expected, the peritectic temperature of the precursor powder increases when Gd content is increased. In all samples, the measurement of T_c using temperature-magnetisation curves exhibits a single superconducting transition. Microstructural and compositional analysis via SEM and EDX analyses indicate further that Y and Gd co-exist in the RE-123 phase matrix. Taken together these results provide strong evidence that a single superconducting phase of combined (Y + Gd)-123 composition is formed and can behave as a solid solution.

Fewer and larger RE-211 inclusions of diameter up to 8 μm are observed in the combined rare earth (Y + Gd)-123 phase matrix via both optical and scanning electron microscopy, even when faster heating profiles are adopted. EDX confirms the presence of a variety of RE-211 phases; Y-211, Gd-211 and (Y–Gd)-211, containing either an inner core of Y-211 and a surrounding Gd-211 layer or vice versa, in these

inclusions. The coarsening mechanism of these RE-211 particles may be due to their favourable growth into one another, resulting in the formation of fewer, and larger particles.

The trapped fields of the combined rare earths bulk superconductors are comparable with those of standard samples containing pure Gd and Y after adjustment of the heating profiles. The formation of large inclusions of (Y–Gd)-211 that are not able to pin magnetic flux effectively explains the lower measured J_c and trapped fields in these samples. It cannot be ruled-out, however, that combining RE in single grains could still improve J_c, although clearly some fine-tuning to reduce the size of the RE-211 inclusions would be required.

In summary, this study has shown that there are no significant difficulties in growing single grains with a combination of Y and Gd elements across the full compositional range. The superconducting properties of these multi-RE element compounds, however, are inferior to those of pure, single-RE element systems due mainly to the presence of larger sized (Y–Gd)-211 particles, which form when mixed rare elements Y and Gd co-exist during the melt process.

Acknowledgments

ORCID iDs

Yunhua Shi ● https://orcid.org/0000-0003-4240-5543
John H Durrell ● https://orcid.org/0000-0003-0712-3102

References

[1] Hull J R 1999 Superconducting bearings *Supercond. Sci. Technol.* **13** R1

[2] John R H 2003 Applications of high-temperature superconductors in power technology *Rep. Prog. Phys.* **66** 1865

[3] Durrell J H *et al* 2014 A trapped field of 17.6 T in melt-processed, bulk Gd–Ba–Cu–O reinforced with shrink-fit steel *Supercond. Sci. Technol.* **27** 082001

[4] Dimos D, Chaudhari P and Mannhart J 1990 Superconducting transport properties of grain boundaries in YBa$_2$Cu$_3$O$_7$ bicrystals *Phys. Rev.* B **41** 4038–49

[5] Durrell J H and Rutter N A 2009 Importance of low-angle grain boundaries in YBa$_2$Cu$_3$O$_{7-\delta}$ coated conductors *Supercond. Sci. Technol.* **22** 013001

[6] Todt V R, Shang X F, Miller D J, St Louis-Weber M and Dravid V P 1996 Controlled growth of bulk bicrystals and the invesigation of microstructure-property relations of YBa$_2$CuO$_x$ grain boundaries *Appl. Phys. Lett.* **69** 3746–8

[7] Miller D J *et al* 1998 Microstructure and transport behavior of grain boundaries in YBa$_2$Cu$_3$O$_y$: a comparison between thin films and bulk bicrystals *Mater. Sci. Eng.* B **53** 125–31

[8] Shi Y, Namburi Kumar D, Zhao W, Durrell J H, Dennis A R and Cardwell D A 2015 The use of buffer pellets to pseudo hot seed (RE)–Ba–Cu–O–(Ag) single grain bulk superconductors *Supercond. Sci. Technol.* **29** 015010

[9] Cardwell D A 1998 Processing and properties of large grain (RE)BCO *Mater. Sci. Eng.* B **53** 1–10

[10] Muralidhar M, Koblischka M R and Murakami M 1999 Embedding of 211 particles in NEG-123 superconductors *Supercond. Sci. Technol.* **12** 555–62

[11] Yamada T, Ikuta H, Itoh Y and Mizutani U 2003 Single domain, *c*-axis oriented (Nd–Eu–Gd)–Ba–Cu–O bulk superconductors *Supercond. Sci. Technol.* **16** 827–31

[12] Hu A, Sakai N and Murakami M 2001 Growth of single-domain (Sm0.5Eu0.5)Ba$_2$Cu$_3$O$_{7-\delta}$ with high T_c and J_c by employing a thermal gradient *Appl. Phys. Lett.* **78** 2539–41

[13] Yoshioka J, Iida K and Murakami M 2001 Study of (Nd, Sm) 422 solid solution and its effect on the melt process of Nd123 bulk superconductors *Physica* C **354** 401–5

[14] Iida K, Muralidhar M and Murakami M 2000 Melt processing of binary (Nd, Eu)–Ba–Cu–O superconductors *Supercond. Sci. Technol.* **13** 683–7

[15] Volochova D 2013 YBCO bulk superconfuctors doped with gadolinium and samarioum *Physica* C **494** 36–40

[16] Setoyama Y *et al* 2014 Systematic change of flux pinning in (Dy, RE)123 and (Y, RE)123 melt-solidified bulks with unit cell orthorhombicity *Supercond. Sci. Technol.* **28** 015014

[17] Volochová D, Diko P, Antal V, Vojtková L and Kováč J 2018 Influence of Gd addition on the microstructure and superconducting properties of YBCO Bulk superconductors *IEEE Trans. Appl. Supercond.* **28** 1–5

[18] Murakami A and Iwamoto A 2019 Mechanical properties of superconducting (Gd, Y)BaCuO large single-grain material fabricated by RE compositional gradient technique *IEEE Trans. Appl. Supercond.* **29** 1–6

[19] Chen Y *et al* 2009 Enhanced flux pinning by BaZrO$_3$ and (Gd, Y)2O$_3$ nanostructures in metal organic chemical vapor deposited GdYBCO high temperature superconductor tapes *Appl. Phys. Lett.* **94** 062513

[20] Chen Y *et al* 2011 Composition effects on the critical current of MOCVD-processed Zr:GdYBCO coated conductors in an applied magnetic field *IEEE Trans. Appl. Supercond.* **21** 3166–70

[21] Zhang S *et al* 2018 Broad temperature study of RE-substitution effects on the in-field critical current behavior of REBCO superconducting tapes *Supercond. Sci. Technol.* **31** 125006

[22] Krabbes G *et al* 2000 Zn doping of YBa$_2$Cu$_3$O$_7$ in melt textured materials: peak effect and high trapped fields *Physica* C **330** 181–90

[23] Hari Babu N, Reddy E S, Cardwell D A, Campbell A M, Tarrant C D and Schneider K R 2003 Artificial flux pinning centers in large, single-grain (RE)–Ba–Cu–O superconductors *Appl. Phys. Lett.* **83** 4806–8

[24] Nariki S, Sakai N, Murakami M and Hirabayashi I 2004 High critical current density in RE–Ba–Cu–O bulk superconductors with very fine RE$_2$BaCuO$_5$ particles *Physica* C **412–414** 557–65

[25] Nariki S, Sakai N and Murakami M 2005 Melt-processed Gd–Ba–Cu–O superconductor with trapped field of 3 T at 77 K *Supercond. Sci. Technol.* **18** S126

[26] Durrell J H *et al* 2014 A trapped field of 17.6 T in melt-processed, bulk Gd–Ba–Cu–O reinforced with shrink-fit steel *Supercond. Sci. Technol.* **27** 082001

[27] Muralidhar M, Jirsa M, Sakai N and Murakami M 2003 Progress in melt-processed (Nd–Sm–Gd)Ba 2 Cu 3 O$_y$ superconductors *Supercond. Sci. Technol.* **16** R1

[28] Dewhurst C D, Wai L and Cardwell D A 1997 Distribution of critical current density in large YBa$_2$Cu$_3$O$_{7-\delta}$ grains fabricated using seeded peritectic solidification *IEEE Trans. Appl. Supercond.* **7** 1925–8

[29] Shi Y, Gough M, Dennis A, Durrell J H and Cardwell D A 2020 Distribution of the superconducting critical current density within a Gd–Ba–Cu–O single grain *Supercond. Sci. Technol.* **33** accepted

[30] Shi Y, Babu N H and Cardwell D A 2005 Development of a generic seed crystal for the fabrication of large grain (RE)–Ba–Cu–O bulk superconductors *Supercond. Sci. Technol.* **18** L13

[31] Shi Y H, Dennis A R and Cardwell D A 2015 A new seeding technique for the reliable fabrication of large, SmBCO single grains containing silver using top seeded melt growth *Supercond. Sci. Technol.* **28** 035014

[32] Yunhua S, Devendra Kumar N, Wen Z, John H D, Anthony R D and David A C 2016 The use of buffer pellets to pseudo hot seed (RE)–Ba–Cu–O–(Ag) single grain bulk superconductors *Supercond. Sci. Technol.* **29** 015010

[33] Shi Y, Namburi D K, Wang M, Durrell J, Dennis A and Cardwell D 2015 A reliable method for recycling (RE)–Ba–Cu–O (RE: Sm, Gd, Y) bulk superconductors *J. Am. Ceram. Soc.* **98** 2760–6

[34] Namburi D K, Shi Y, Palmer K G, Dennis A R, Durrell J H and Cardwell D A 2016 An improved top seeded infiltration growth method for the fabrication of Y–Ba–Cu–O bulk superconductors *J. Eur. Ceram. Soc.* **36** 615–24

[35] Hatano T, Matsushita A, Nakamura K, Sakka Y, Matsumoto T and Ogawa K 1987 Superconducting and transport properties of B–Y–Cu–O compounds -orthorhombic and tetragonal phases *Japan. J. Appl. Phys.* **26** L721–3

[36] Chen D X and Goldfarb R B 1989 Kim model for magnetization of type-II superconductors *J. Appl. Phys.* **66** 2489–500

[37] Cardwell D A, Shi Y H, Hari Babu N, Pathak S K, Dennis A R and Iida K 2010 Top seeded melt growth of Gd–Ba–Cu–O single grain superconductors *Supercond. Sci. Technol.* **23** 034008

[38] Congreve J V J, Shi Y, Dennis A R, Durrell J H and Cardwell D A 2016 Improvements in the processing of large grain, bulk Y–Ba–Cu–O superconductors via the use of additional liquid phase *Supercond. Sci. Technol.* **30** 015017

[39] Volochová D *et al* 2012 Growth of Y123 bulk crystals in Y1.5Ba2Cu$_3$O$_x$ system with CeO$_2$ addition *J. Cryst. Growth* **353** 31–4

[40] Thoma M, Shi Y, Dennis T, Durrell J and Cardwell D 2015 Effect of Y-211 particle size on the growth of single grain Y–Ba–Cu–O bulk superconductors *J. Cryst. Growth* **412** 31–9

[41] Endo A, Chauhan H S, Egi T and Shiohara Y 1996 Macrosegregation of Y$_2$Ba$_1$Cu$_1$O$_5$ particles in Y$_1$Ba$_2$Cu$_3$O$_{7-\delta}$ crystals grown by an undercooling method *J. Mater. Res.* **11** 795–803

[42] Izumi T, Nakamura Y and Shiohara Y 2011 Doping effects on coarsening of Y$_2$BaCuO$_5$ phase in liquid *J. Mater. Res.* **8** 1240–6

[43] Shi Y *et al* 2012 Synthesis of YBa$_2$Cu$_3$O$_{7-\delta}$ and Y$_2$BaCuO$_5$ nanocrystalline powders for YBCO superconductors using carbon nanotube templates *ACS Nano* **6** 5395–403

[44] Langhorn J B, Black M A and McGinn P J 1998 Effect of mixing Nd, Eu, and Gd rare earth elements on RE-cuprate high-T_c superconductors *J. Supercond.* **11** 581–5